

Original Research

# Quantitative Proteomics Reveals Neuroprotective Mechanism of Ginkgolide B in $A\beta_{1-42}$ -induced N2a Neuroblastoma Cells

Yidan Zhang<sup>1</sup>, Yuan Zhao<sup>1</sup>, Jian Zhang<sup>1</sup>, Ya Gao<sup>1</sup>, Shuyue Li<sup>1</sup>, Cui Chang<sup>1</sup>,  
Guofeng Yang<sup>1,\*</sup> <sup>1</sup>Department of Geriatrics, The Second Hospital of Hebei Medical University, 050000 Shijiazhuang, Hebei, China\*Correspondence: [gf\\_yang71@126.com](mailto:gf_yang71@126.com) (Guofeng Yang)

Academic Editor: Gernot Riedel

Submitted: 7 August 2022 Revised: 5 September 2022 Accepted: 6 September 2022 Published: 14 February 2023

## Abstract

**Objective:** Ginkgolide B (GB) possesses anti-inflammatory, antioxidant, and anti-apoptotic properties against neurotoxicity induced by amyloid beta ( $A\beta$ ), but the potential neuroprotective effects of GB in Alzheimer's therapies remain elusive. We aimed to conduct proteomic analysis of  $A\beta_{1-42}$  induced cell injury with GB pretreatment to uncover the underlying pharmacological mechanisms of GB. **Methods:** Tandem mass tag (TMT) labeled liquid chromatography-tandem mass spectrometry (LC-MS/MS) method was applied to analyze protein expression in  $A\beta_{1-42}$  induced mouse neuroblastoma N2a cells with or without GB pretreatment. Proteins with fold change  $>1.5$  and  $p < 0.1$  from two independent experiments were regarded as differentially expressed proteins (DEPs). Gene ontology (GO) and Kyoto Encyclopedia of Genes and Genomes (KEGG) enrichment analyses were performed to analyze the functional annotation information of DEPs. Two key proteins osteopontin (SPP1) and ferritin heavy chain 1 (FTH1) were validated in another three samples using western blot and quantitative real-time PCR. **Results:** We identified a total of 61 DEPs in GB treated N2a cells, including 42 upregulated and 19 downregulated proteins. Bioinformatic analysis showed that DEPs mainly participated in the regulation of cell death and ferroptosis by down-regulating SPP1 protein and up-regulating FTH1 protein. **Conclusions:** Our findings demonstrate that GB treatment provides neuroprotective effects on  $A\beta_{1-42}$  induced cell injury, which may be related to the regulation of cell death and ferroptosis. The research puts forward new insights into the potential protein targets of GB in the treatment of Alzheimer's disease (AD).

**Keywords:** Alzheimer's disease; Ginkgolide B; tandem mass tag; bioinformatics analysis; ferroptosis; cell death

## 1. Introduction

Alzheimer's disease (AD) is the commonest neurodegenerative disorder in the older people accompanied by progressive cognitive impairment and behavior dysfunction. Approximately 3.2% of the population over 65 years old suffers AD, and the global prevalence will reach 115 million sufferers by 2050 [1]. The typical pathological features are extracellular aggregated senile plaques of amyloid beta ( $A\beta$ ) and intracellular highly phosphorylated neurofibrillary tau tangles in the cerebrum [2]. Abnormal accumulation of  $A\beta$  within the cerebrum is an initial pathological change of AD, which appears years or more than a decade ahead of the onset of clinical symptoms [3]. An imbalance between  $A\beta$  generation by neurons and clearance from the interstitial fluid results in extracellular amyloid plaques deposition [4], accompanied by the resultant neuroinflammation, oxidative stress, free radical damage, and extensive neuron death [5]. Membrane-spanning protein amyloid precursor protein (APP) is cleaved to  $A\beta_{1-40}$  peptide and  $A\beta_{1-42}$  peptide by  $\beta$ -secretase and  $\gamma$ -secretase [6].  $A\beta_{1-42}$  peptide is more hydrophobic and tends to aggregate to form an oligomeric or fibrous structure which is the core component of senile plaques [7]. Cells with neurotoxic  $A\beta_{1-42}$  peptide intervention could replicate the pathologi-

cal hallmarks of AD. Therefore, the *in vitro*  $A\beta_{1-42}$ -treated mouse neuroblastoma N2a cell line is considered a classical model to mimic the cell injury of AD, which can be used for exploring the underlying pathological mechanism of AD.

Phytochemicals are bioactive substances of plant origin with various structures and significant pharmaceutical properties [8]. Ginkgolide B (GB,  $C_{20}H_{24}O_{10}$ , molecular weight = 424.3986 g/mol) is a kind of diterpenoids isolated from the leaves of Ginkgo biloba, and has various pharmacological effects, such as inhibiting platelet activating [9], scavenging oxygen free radicals [10], and antioxidative stress function. GB could prevent neuronal cell injury caused by oxidative stress *in vitro* and improve cognitive function in the central nervous system [11]. GB also possesses neuroprotective functions against cerebral ischemic injury and  $A\beta$ -induced neurotoxicity through various biological properties of anti-inflammation, antioxidative stress, and anti-apoptosis [12–14]. However, its specific pharmacological mechanism in AD remains ambiguous. In the current study, we aim to explore the protective effects of GB on cell injury caused by  $A\beta_{1-42}$  and uncover its underlying cellular mechanisms.

Mass spectrometry (MS)-based quantitative proteomics is an advanced technology for unbiased protein identification and quantitation on a large scale, which re-



lies on precise, high-throughput, and reproducible techniques [15]. Advances in liquid chromatography-tandem MS (LC-MS/MS) have qualified for the identification and quantification of thousands of proteins in biological samples. It not only identifies proteins in normal and pathological states, but also accurately quantifies their abundance [16]. LC-MS/MS technique has significant value in identifying functional modules and pathways, discovering biomarkers, as well as diagnosing and surveilling diseases. LC-MS/MS technology with stable isotope-labeling amino acids has been extensively applied for exploring the targets and mechanisms of multiple diseases and drugs.

Therefore, tandem mass tag (TMT) labeled LC-MS/MS-based quantitative proteomic analysis of proteins from GB treated N2a cells was performed to analyze the differentially expressed proteins (DEPs) that are associated with the neuroprotective mechanism of GB. As a result, 61 proteins were identified as DEPs (fold change  $>1.5$  and  $p < 0.1$ ). Of these, 42 proteins were upregulated and 19 proteins were downregulated after GB treatment. Gene ontology (GO) and Kyoto Encyclopedia of Genes and Genomes (KEGG) enrichment analyses revealed that DEPs mainly involved in the regulation of cell death, immune system process, and ferroptosis. Among the DEPs, two key proteins ferritin heavy chain 1 (FTH1) and osteopontin (SPP1), mainly participate in the regulation of cell death and ferroptosis, were verified using western blot and quantitative real-time PCR (qRT-PCR). The current conclusions provide new insight into the potential therapeutic targets of GB in AD.

## 2. Materials and Methods

### 2.1 Preparation of GB Stock Solutions

GB (HPLC purity  $>98\%$ ) was purchased from Chengdu Pufei De Biotech Co., Ltd. Its molecular weight is 424.3986 g/mol and molecular formula is  $C_{20}H_{24}O_{10}$  (Fig. 1c). It was dissolved in dimethyl sulfoxide (DMSO, Sigma, St. Louis, MO, USA) and prepared in a stock solution of 5 mmol/L with culture medium. The stock solution was diluted to required concentrations with the same culture before use. DMSO concentration was kept below 0.1% to prevent cytotoxic reaction [17].

### 2.2 Preparation of $A\beta_{1-42}$ Oligomers

The preparation of  $A\beta_{1-42}$  oligomers was based on a widely recognized method [18,19]. 1 mg lyophilized  $A\beta_{1-42}$  peptide (AS-20276; AnaSpec, Shanghai, China) was dissolved in 221  $\mu$ L of 100% hexafluoroisopropanol at a concentration of 1 mM and evenly divided into two tubes. Then, the peptide film was dried under vacuum. Approximately 0.5 mg dried peptide film was redissolved in 20  $\mu$ L of fresh dry DMSO to a concentration of 5 mM and diluted with F12 cell culture medium to 100  $\mu$ M [17]. The solution was incubated at 4  $^{\circ}$ C for 24 h and centrifuged at 14,000  $\times g$  at 4  $^{\circ}$ C for 10 min for elimination of fibrils. The su-

pernatant that consists of soluble oligomerized  $A\beta_{1-42}$  was used for experiments.

### 2.3 Transmission Electron Microscopy (TEM)

Oligomerized  $A\beta_{1-42}$  was identified by means of TEM. Briefly, 10  $\mu$ L of  $A\beta_{1-42}$  oligomers was added to copper mesh grids with formvar coating and carbon stabilizing for 1 min.  $A\beta_{1-42}$  oligomers were stained with 5  $\mu$ L of 1% uranyl acetate for 30 s using negative staining technique [17]. The completely dried grids were observed using a 200 kV electron microscope (Tecnai G2 20 Twin, FEI, Czech Republic).

### 2.4 Cell Culture and Treatments

The mouse neuroblastoma N2a cells were donated by Ji Jianguo Lab (the State Key laboratory of Protein and Plant Gene Research, College of Life Sciences, Peking University) and cultured in Dulbecco's Modified Eagle Medium (DMEM, Hyclone, Logan, UT, USA) containing 10% fetal bovine serum (Hyclone, Logan, UT, USA). N2a cells were maintained in a humidified atmosphere containing 5%  $CO_2$  at 37  $^{\circ}$ C. The cells were pretreated with GB or vehicle for 2 h, followed by incubation in the presence or absence of 10  $\mu$ M  $A\beta_{1-42}$  oligomers for an additional 24 h. The experiments involve the control group (treated with 0.1% DMSO for 24 h), the  $A\beta$  group (treated with 10  $\mu$ M  $A\beta_{1-42}$  for 24 h) and the  $A\beta$  + GB group (pretreated with 100  $\mu$ M GB for 2 h followed by 10  $\mu$ M  $A\beta_{1-42}$  for 24 h).

### 2.5 Detection of Cell Survival Rates

Cell survival rates were tested by a colorimetric 3-(4,5-dimethylthiazol-2-yl)-2,5-diphenyl-tetrazolium bromide (MTT) assay (Beyotime Biotechnology, Shanghai, China). N2a cells were seeded in 96-well plates and treated according to the experiment designed when the cells reached to 60% confluence. Then the cells were incubated with 10  $\mu$ L MTT (5 mg/mL) at 37  $^{\circ}$ C for 4 h, and the MTT formazan was extracted with 150  $\mu$ L DMSO. The absorbance of each well was measured at 570 nm using a Multiskan FC microtiter plate reader (Thermo Fisher Scientific, Waltham, MA, USA).

### 2.6 Flow Cytometry Analysis of Cell Apoptosis

Apoptotic N2a cells were determined using Annexin V-fluorescein isothiocyanate (FITC)/propidium iodide (PI) cell apoptosis detection kit (TransGen Biotech Co, Beijing, China). After treatments, N2a cells were digested with trypsin, washed, and resuspended in Annexin V binding buffer. Then, cells were incubated with 5  $\mu$ L of Annexin V-FITC and 5  $\mu$ L of PI at room temperature for 15 min in the dark. The number of apoptotic cells were detected using a flow cytometer (FACSVerse, BD Biosciences, Franklin, NJ, USA) and analyzed using FlowJo software (Version 7.6, TreeStar Inc, San Carlos, CA, USA).

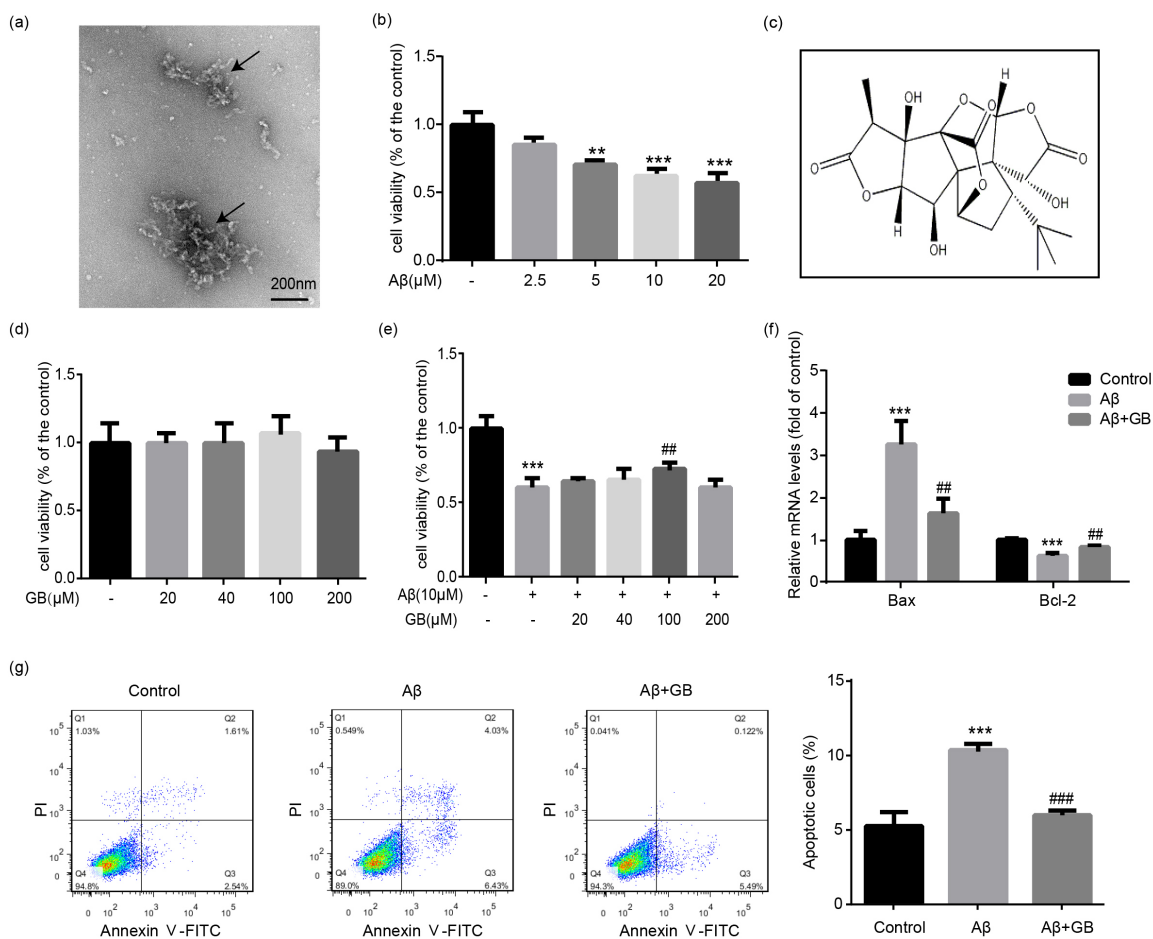


**Fig. 1. Effect of Ginkgolide B (GB) on  $A\beta_{1-42}$ -induced cytotoxicity in N2a neuroblastoma cells.** (a) The TEM images of  $A\beta_{1-42}$  oligomers via negative staining. (b) N2a cells were treated with 0, 2.5, 5, 10 and 20  $\mu\text{M}$   $A\beta_{1-42}$  oligomers for 24 h, and the cell survival rates were then measured by MTT assay ( $n = 5$ ). (c) The chemical structure of GB. (d) Cells were treated with GB at various concentrations (0, 20, 40, 100 and 200  $\mu\text{M}$ ) for 24 h, and the cell viability was measured by MTT assay ( $n = 5$ ). (e) Cells were pretreated with various concentrations of GB (0, 20, 40, 100 and 200  $\mu\text{M}$ ) for 2 h, followed by incubation with 10  $\mu\text{M}$   $A\beta_{1-42}$  oligomers for another 24 h. Cell survival rates were measured by MTT assay ( $n = 5$ ). (f) Bax and Bcl-2 mRNA levels determined by quantitative PCR (qPCR) ( $n = 3$ ). (g) The number of apoptotic cells in the existence of  $A\beta_{1-42}$  oligomers and GB analyzed by flow cytometry. Quantified apoptotic cells in all groups ( $n = 3$ ). Data were presented as mean  $\pm$  SEM. \*\* $p < 0.01$  and \*\*\* $p < 0.001$  vs. control group; ## $p < 0.01$  and ### $p < 0.001$  vs.  $A\beta$  group.

### 2.7 Measurement of Intracellular Reactive Oxygen Species (ROS)

Intracellular ROS levels of N2a cells were tested using ROS probe 2',7'-dichlorofluorescein diacetate (DCFH-DA) (Beyotime Biotechnology, Nanjing, China). After treatment, N2a cells were incubated with 10  $\mu\text{M}$  DCFH-DA for 30 min and then washed with serum-free cell culture medium. The DCF fluorescence was quantified using a multimode microplate reader with an excitation source at 485 nm and an emission at 530 nm. The values were expressed as the fold of control.

### 2.8 Measurement of Superoxide Dismutase (SOD) Activity and Malondialdehyde (MDA) Content

The SOD activity and MDA content were detected using commercially available kits (Nanjing Jiancheng Bio-engineering Institute, Nanjing, China) following the protocols. The SOD activity was tested using the xanthine oxidase method and measured by the absorbance of superoxide anion free radical at 550 nm. The lipid peroxidation level was reflected by MDA concentrations using the thibaburic acid (TBA) method. MDA concentrations were measured by the absorbance of TBA reactive substances at 532 nm.

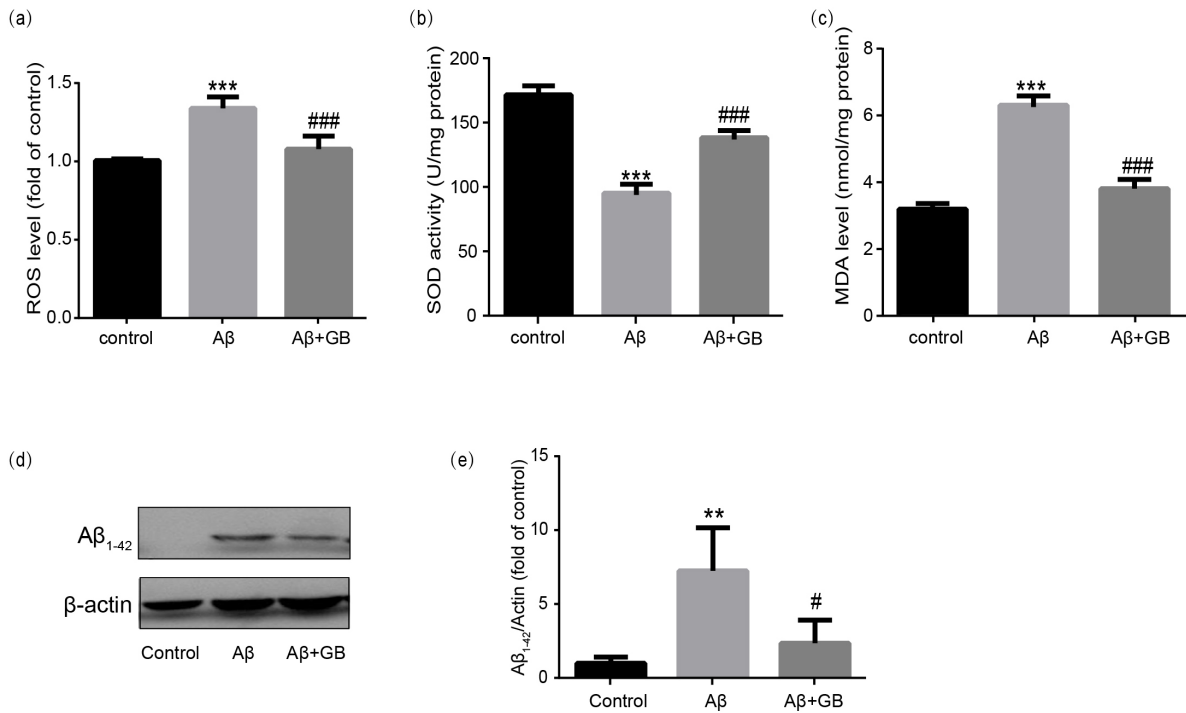


**Fig. 2. Effect of Ginkgolide B (GB) on  $A\beta_{1-42}$ -induced oxidative stress in N2a cells.** The relative ROS level (a), SOD activity (b) and MDA content (c) from all experimental groups were measured using commercial kits (n = 5). (d,e) Representative images of  $A\beta_{1-42}$  peptide levels and relative level normalized to  $\beta$ -actin (n = 3). Data were presented as mean  $\pm$  SEM. \*\* $p < 0.01$  and \*\*\* $p < 0.001$  vs. control group; # $p < 0.05$  and ### $p < 0.001$  vs.  $A\beta$  group.

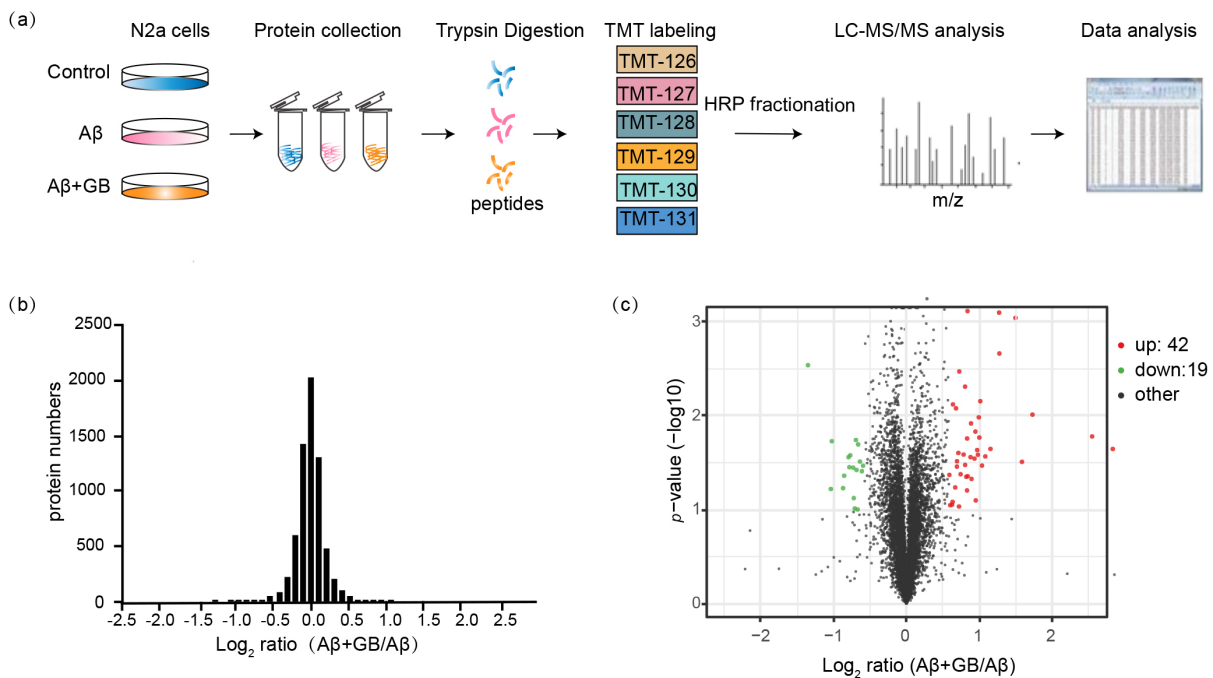


**Fig. 3. Global proteome profiling of N2a cells with GB pretreatment.** (a) Experimental workflow for proteomic analysis of N2a cells. (b) The relative abundance ratios distribution of quantified 6740 proteins in GB treated N2a cells by proteomics. Proteins ratios ( $A\beta + GB/A\beta$ ) were presented on the log2 scale. (c) Volcano plot of quantified proteins was represented as the fold change ( $\log_2$ ) and the  $p$  value ( $-\log_{10}$ ). The criterion for determining DEPs is fold change  $> 1.5$  and  $p$  value  $< 0.1$ . Red dots are upregulated proteins, and blue plots are downregulated proteins.

**Table 1. Effects of GB on A $\beta$ -induced differentially expressed proteins.**

No	Accession	Gene name	Description	GB/A $\beta$	Ratio	<i>p</i> value
1	O08600	Endog	Endonuclease G, mitochondrial	UP	1.7890	0.0008
2	E9Q414	Apob	Apolipoprotein B-100	UP	2.4161	0.0008
3	P09528	Fth1	Ferritin heavy chain 1	UP	2.8239	0.0009
4	P32261	Serpinc1	Antithrombin-III	UP	2.4223	0.0022
5	Q61838	Pzp	Pregnancy zone protein	UP	1.6535	0.0034
6	Q8BU04	Ubr7	Putative E3 ubiquitin-protein ligase UBR7	UP	1.7480	0.0049
7	P13011	Scd2	Acyl-CoA desaturase 2	UP	2.0205	0.0070
8	P07742	Rrm1	Ribonucleoside-diphosphate reductase large subunit	UP	1.5571	0.0075
9	P19221	F2	Prothrombin	UP	1.6033	0.0083
10	Q9CPX4	Ftl1	Ferritin	UP	3.3193	0.0097
11	P11276	Fn1	Fibronectin	UP	1.9921	0.0104
12	Q9D1C1	Ube2c	Ubiquitin-conjugating enzyme E2 C	UP	1.8494	0.0121
13	O88668	Creg1	Protein CREG1	UP	1.9284	0.0147
14	P02802	Mt1	Metallothionein-1	UP	5.8565	0.0166
15	P53996	Cnbp	Cellular nucleic acid-binding protein	UP	2.0013	0.0170
16	Q9D0J8	Ptms	Parathymosin	UP	1.7816	0.0174
17	Q61704	Itih3	Inter-alpha-trypsin inhibitor heavy chain H3	UP	2.2255	0.0225
18	P02798	Mt2	Metallothionein-2	UP	7.1289	0.0226
19	P26350	Ptma	Prothymosin alpha	UP	1.9612	0.0232
20	Q9ESY9	Ifi30	Gamma-interferon-inducible lysosomal thiol reductase	UP	1.6397	0.0249
21	G5E911	Fam3c	DNA segment, Chr 6, Wayne State University 176, expressed, isoform CRA_f	UP	1.7230	0.0259
22	V9GX81	Mroh6	Maestro heat-like repeat family member 6	UP	1.9743	0.0260
23	Q6GQT1	A2m	Alpha-2-macroglobulin-P	UP	2.1189	0.0271
24	P29699	Ahsg	Alpha-2-HS-glycoprotein	UP	1.8409	0.0276
25	Q9DBX1	Rgcc	Regulator of cell cycle RGCC	UP	1.9121	0.0286
26	A0A140L134	Zfp654	Zinc finger protein 654	UP	1.6178	0.0305
27	P01029	C4b	Complement C4-B	UP	3.0035	0.0309
28	Q91W10	Slc39a8	Zinc transporter ZIP8	UP	1.7485	0.0334
29	P06684	C5	Complement C5	UP	2.0535	0.0339
30	Q8VDF2	Uhrf1	E3 ubiquitin-protein ligase UHRF1	UP	1.6168	0.0348
31	Q8BVE8-2	Nsd2	Isoform 2 of Histone-lysine N-methyltransferase NSD2	UP	1.6752	0.0419
32	Q9Z2G0	Fem1b	Protein fem-1 homolog B	UP	1.5050	0.0426
33	Q9WUQ5	Cxcl14	C-X-C motif chemokine 14	UP	1.7908	0.0440
34	Q8K0E8	Fgb	Fibrinogen beta chain	UP	1.7678	0.0447
35	Q3UA16	Spc25	Kinetochore protein Spc25	UP	1.8590	0.0471
36	Q80V24	Vgll4	Transcription cofactor vestigial-like protein 4	UP	1.5912	0.0580
37	Q3UU35	Ovos	Ovostatin homolog	UP	1.7804	0.0624
38	P54843-2	Maf	Isoform 2 of Transcription factor Maf	UP	1.9349	0.0798
39	P22272	Il6ra	Interleukin-6 receptor subunit alpha	UP	1.5519	0.0826
40	Q9WTN3	Srebf1	Sterol regulatory element-binding protein 1	UP	1.5448	0.0886
41	Q80YQ1	Thbs1	Thrombospondin-1	UP	1.5171	0.0897
42	Q9QZI9	Serinc3	Serine incorporator 3	UP	1.6498	0.0926
43	P04441-2	Cd74	Isoform Short of H-2 class II histocompatibility antigen gamma chain	DOWN	0.6207	0.0005
44	Q9Z0J7	Gdf15	Growth/differentiation factor 15	DOWN	0.3918	0.0029
45	Q9D154	Serp1b1a	Leukocyte elastase inhibitor A	DOWN	0.6184	0.0181
46	Q64339	Isg15	Ubiquitin-like protein ISG15	DOWN	0.4915	0.0186
47	A0A0B4J1E6	Fcgr2b	Fc receptor, IgG, low affinity IIb	DOWN	0.6316	0.0202
48	P04117	Fabp4	Fatty acid-binding protein, adipocyte	DOWN	0.5860	0.0264
49	Q9CYL5	Glipr2	Golgi-associated plant pathogenesis-related protein 1	DOWN	0.5763	0.0276
50	A6H5X4	Phf11	PHD finger protein 11	DOWN	0.6428	0.0307
51	P49813	Tmod1	Tropomodulin-1	DOWN	0.6621	0.0340

**Table 1. Continued.**

No	Accession	Gene name	Description	GB/A $\beta$	Ratio	p value
52	O35368-3	Ifi203	Isoform 3 of Interferon-activable protein 203	DOWN	0.5812	0.0353
53	Q3U4P5	Psen2	Presenilin	DOWN	0.6028	0.0357
54	A0A0R4J0G6	Qpct	Glutaminyl-peptide cyclotransferase	DOWN	0.6221	0.0378
55	Q3TRM8	Hk3	Hexokinase-3	DOWN	0.6545	0.0389
56	F8WIP8	Spp1	Osteopontin	DOWN	0.5529	0.0435
57	P11152	Lpl	Lipoprotein lipase	DOWN	0.5473	0.0590
58	O88935	Syn1	Synapsin-1	DOWN	0.4871	0.0603
59	Q9Z1R3	Apom	Apolipoprotein M	DOWN	0.6059	0.0754
60	Q8C9S4	Ccdc186	Coiled-coil domain-containing protein 186	DOWN	0.6117	0.0973
61	Q9WTR6	Slc7a11	Cystine/glutamate transporter	DOWN	0.6284	0.0997

### 2.9 Protein Digestion and TMT Labeling

The proteins of N2a cells were precipitated in pre-chilled ( $-20^{\circ}\text{C}$ ) trichloroacetic acid and acetone. The precipitated proteins were then dissolved in 8 M urea buffer, reduced with 100 mM dithiothreitol (Sigma Aldrich, Saint Louis, MO, USA), and alkylated with 200 mM iodoacetamide (Sigma Aldrich, Saint Louis, MO, USA). Protein digestion took place in the existence of Lys-C (1:1000,  $37^{\circ}\text{C}$  for 3 h) and trypsin (1:50,  $37^{\circ}\text{C}$  for 8–18 h) [20], and this reaction was terminated with trifluoroacetic acid (TFA). The peptide mixtures were transferred to C18 Extraction Disks (Empore3M, Agilent Technologies, Sant Clara, CA, USA) and sequentially flushed with anhydrous acetonitrile (ACN), 0.1% TFA/70% ACN, and 0.1% TFA for desalination. Peptides were then vacuum dried and dissolved in 100 mM tetraethylammonium bicarbonate buffer. Each sample (40  $\mu\text{g}$  peptides) were labeled using six-plex TMT reagents (90061, Thermo Scientific, Waltham, MA, USA) with ACN buffer for 60 min at room temperature [17]. Peptides derived from the control group, A $\beta$  group and A $\beta$  + GB group were labeled with 126 and 127 TMT tags, 128 and 129 TMT tags, 130 and 131 TMT tags, respectively. The labeling reaction was terminated by 8  $\mu\text{L}$  of 5% hydroxylamine (20 min, room temperature). TMT-labeled peptide mixture was loaded on the C18 extraction disk cartridge and eluted by gradient acetonitrile (10%, 12.5%, 15%, 17.5%, 20%, 22.5%, 25%, and 50%). The fractionated peptides (10% and 50%) were pooled into one fraction, leaving seven fractions in the TMT experiment. These fractions were vacuum dried for subsequent LC-MS/MS measurement.

### 2.10 LC-MS/MS Analysis

TMT-labeled peptides were analyzed on an Orbitrap Fusion Lumos Tribrid instrument (Thermo Scientific). Peptides were dissolved in 0.2% formic acid, detached in mobile phase containing 0.1% formic acid and eluted using a nonlinear 194 min acetonitrile gradient of 6%–90% buffer (0.1% formic acid with 80% acetonitrile) at 300 nL/min. The settings of MS parameters were as follows: MS1 resolution at 120,000, mass scan of 300–1500 m/z, automatic gain control (AGC) target at  $1 \times 10^6$ , maximum injection

time at 100 ms, and 30% of radio frequency, MS2 mass resolution at 50,000, high-energy collision dissociation for MS/MS, 37% of collision energy, normalized AGC target at  $1 \times 10^5$ , 1.2 m/z isolation width, 30 s dynamic exclusion [17].

### 2.11 Database Search Parameters

Protein identification, quantification, and MS/MS original data were analyzed by SEQUEST search algorithm using Proteome Discoverer (version 2.2, Thermo Scientific, Waltham, MA, USA). Raw files were searched with a mouse Uniprot protein database. Search criteria included maximum missed trypsin cleavages of 2; fixed modification on lysine and N-terminus for TMT six-plex tags; dynamic modification for oxidation of methionine residues; carbamidomethyl on cysteines; mass tolerance of 10 ppm; 0.05 Da for MS/MS tolerance; 1% false discovery rate (FDR) [21,22]; and 1% FDR at peptide and protein levels [17]. Reporter ion intensities was normalized using the index of total reporter ion intensity.

### 2.12 Data Analysis and Interpretation

The protein ratios (A $\beta$  + GB/A $\beta$ ) were normalized in the transformed Log<sub>2</sub> fold change to adjust the unequal protein content. *p*-value was calculated with an independent student's *t*-test (A $\beta$  + GB versus A $\beta$ ). Proteins with a cut-off of *p* < 0.1 and fold change > 1.5 from two independent experiments were regarded as DEPs.

### 2.13 KEGG and GO Enrichment Analyses of DEPs

The Database for Annotation, Visualization, and Integrated Discovery (DAVID) is an online database that offers systematic and comprehensive functional annotation information of proteins and genes to reveal biological information [23,24]. KEGG pathway enrichment analysis and GO analysis (biological process, molecular function, and cellular component) of DEPs were carried out using DAVID (version 6.8) to analyze the function of DEPs. *p* < 0.05 was regarded as statistical significance.

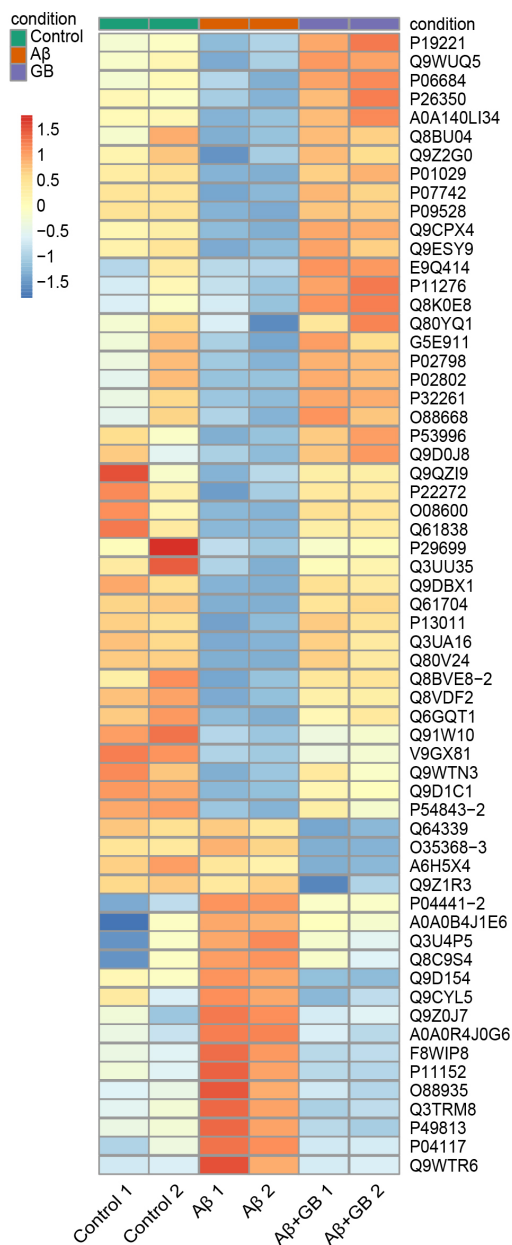


**Fig. 4. Hierarchical clustering analysis of the DEPs in N2a cells with GB pretreatment.** The map reflects the relative abundance ratios ( $A\beta + GB/A\beta$ ). Red squares indicate high expression proteins, and blue squares indicate low expression proteins.

#### 2.14 Western Blot

N2a cells were lysed in 1% sodium dodecyl sulfate using an ultrasound homogenizer. Protein concentration was quantitatively measured using a Pierce™ BCA Protein Assay Kit (Thermo Fisher Scientific). Equal amounts of protein (15  $\mu$ g) were loaded in to each lane of 10% sodium dodecyl sulfate-polyacrylamide gel electrophoresis and transferred to a polyvinylidene fluoride membranes using a semidry blotting apparatus (Bio-Rad, Hercules, CA, USA). The membranes were blocked with 5% non-fat milk and incubated with primary antibodies overnight

at 4 °C: anti-FTH1 (1:1000; ab63856, Abcam, Cambridge, UK), anti-SPP1 (1:1000; ab218237, Abcam), anti- $A\beta_{1-42}$  (1:1000; 14974, Cell Signaling, Boston, MA, USA), and anti- $\beta$ -actin (1:2000; ab3280, Abcam). After washing, the membranes were then incubated with horseradish peroxidase (HRP)-conjugated secondary antibodies (4050-05 or 1031-05, Southern Biotech, Birmingham, AL, USA) for 1 h at room temperature. Subsequently, the Protein bands were detected using Immobilon Western Chemiluminescent HRP substrate (Millipore, Billerica, MA, USA), and images were scanned using X-ray films. Kodak Digital Science 1D software (Eastman Kodak Company, Rochester, NY, USA) was used to analysis the sum optical density.

#### 2.15 Quantitative Real-Time PCR Assay

Total RNA was extracted from N2a cells using Trizol reagent (Invitrogen, Carlsbad, CA, USA) following the supplier's recommendations. Total RNA (1.5  $\mu$ g) was reversely transcribed to cDNA using a HiFi-Script cDNA Synthesis kit (CW Bio, Beijing, China). Quantitative analysis of FTH1 and SPP1 expressions was performed using CFX96™ Real Time PCR Detection System (Bio-Rad, Hercules, CA, USA). The mRNA levels were calculated using the  $2^{-\Delta\Delta CT}$  algorithm and normalized to GAPDH. The primers in this article were as follows: SPP1, Forward (5'->3'): AGCAAGAACTCTTCCAAGCAA, Reverse (5'-3'): GTGAGATTCGTCAGATTCATCCG. FTH1, Forward (5'-3'): TAAAGAAACCAGACCGTGATGACT, Reverse (5'-3'): TGCAGTTCAGTAGTGACTGATTC. GAPDH, Forward (5'-3'): GGTCGGTGTGAACGGATTT, Reverse (5'-3'): GTGGATGCAGGGATGATGTT.

#### 2.16 Statistical Analysis

All data were shown as mean  $\pm$  SEM and analyzed by one-way analysis of variance (ANOVA) followed by Student-Newman-Keuls test for intergroup comparisons. All analyses were conducted using SPSS statistical software (Version 17.0, SPSS, Chicago, IL, USA). A  $p$  value  $< 0.05$  was identified as statistical significance.

### 3. Results

#### 3.1 GB Alleviated $A\beta_{1-42}$ -Induced Cytotoxicity in N2a Cells

The  $A\beta_{1-42}$ -injured N2a cell model was established in the present study. The characteristic of  $A\beta_{1-42}$  oligomers was revealed by TEM (Fig. 1a), and the toxicity of  $A\beta_{1-42}$  oligomers was tested by MTT assay. The MTT results showed a dose-dependent association between  $A\beta_{1-42}$  concentration and cell injury. 10  $\mu$ M  $A\beta_{1-42}$  treatment markedly decreased cell survival rate compared with the control group (Fig. 1b). However, 20  $\mu$ M  $A\beta_{1-42}$  produced no notable changes in cell viability compared with 10  $\mu$ M  $A\beta_{1-42}$  (Fig. 1b,  $p > 0.05$ ). Therefore,  $A\beta_{1-42}$  oligomers at a concentration of 10  $\mu$ M was chosen for  $A\beta$ -

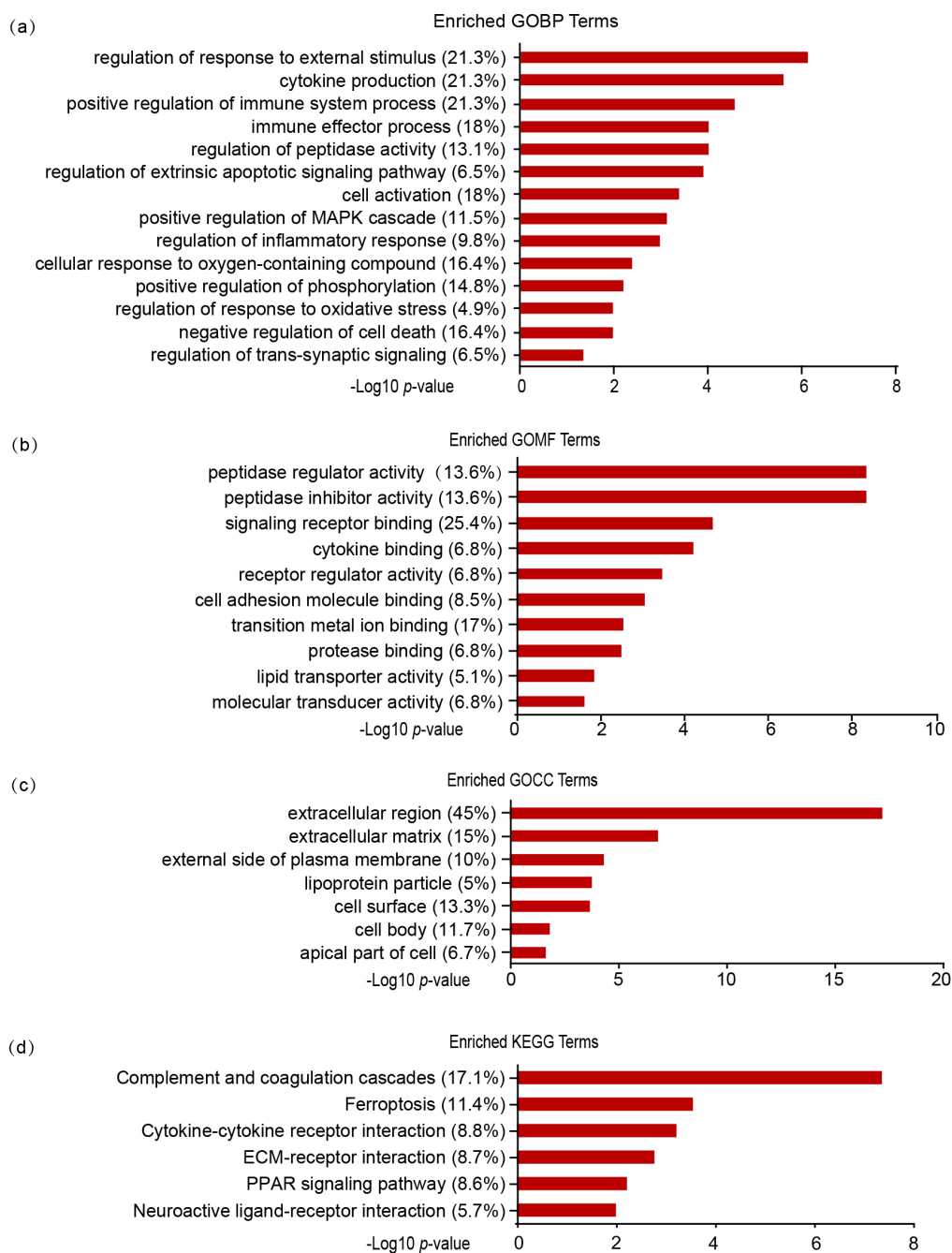


**Fig. 5. GO and KEGG enrichment analyses of DEPs.** GO enrichment analysis of DEPs in three categories: biological process (a), molecular function (b), and cellular component (c). (d) KEGG pathway enrichment analysis of DEPs. The percentages indicate the enriched proteins among all DEPs. *p* value indicates significantly enriched terms.

induced cell model. GB, a kind of diterpenoids isolated from the leaves of Ginkgo biloba, provides neuroprotective functions against  $A\beta$ -induced neurotoxicity in previous studies [14]. To verify whether GB exerts any effect on N2a cells themselves, the viability of various concentrations of GB intervened N2a cells was detected. GB (20–200  $\mu$ M) alone caused no obvious effects on cell viability, with the maximal cell viability occurring at 100  $\mu$ M (Fig. 1d). GB (20–200  $\mu$ M) pretreatment showed certain inhibitory effect

on cell injury caused by  $A\beta_{1-42}$  oligomers, especially at a concentration of 100  $\mu$ M (Fig. 1e). Hence, 100  $\mu$ M GB was used for further experiments.

### 3.2 GB Relieved $A\beta_{1-42}$ -Induced Apoptosis in N2a Cells

The functions of GB on cell apoptosis stimulated by  $A\beta_{1-42}$  oligomers were measured by Annexin V-FITC/PI staining and flow cytometry. Cells incubated with  $A\beta_{1-42}$  alone showed the highest apoptosis rate (10.46%), and the

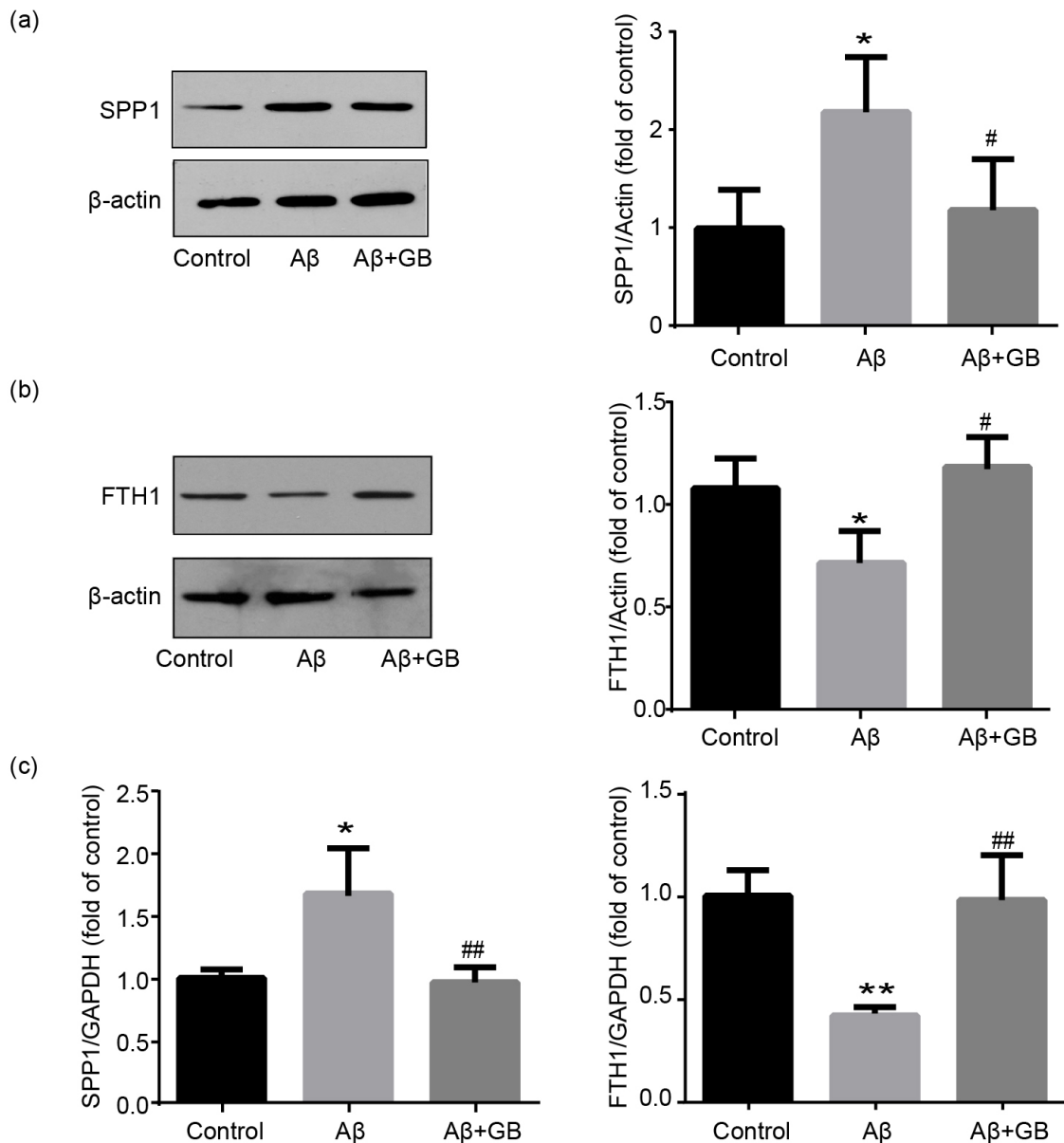


**Fig. 6. Validation of SPP1 and FTH1 expression levels in N2a cells.** (a) Representative images of SPP1 protein levels and relative level normalized to  $\beta$ -actin (n = 3). (b) Representative images of FTH1 protein levels and relative level normalized to  $\beta$ -actin (n = 3). (c) Relative mRNA levels of SPP1 and FTH1 determined by qPCR (n = 3). Data was expressed as mean  $\pm$  SEM. \* $p$  < 0.05 and \*\* $p$  < 0.01 vs. control group; # $p$  < 0.05 and ## $p$  < 0.01 vs. A $\beta$  group.

apoptosis rate was significantly reduced with 100  $\mu$ M GB treatment (5.61%) (Fig. 1g). GB also alleviated A $\beta_{1-42}$ -induced elevation of Bax expression and downregulation of Bcl-2 level (Fig. 1f). These results showed that GB relieved cell apoptosis caused by A $\beta_{1-42}$  oligomers.

### 3.3 GB Attenuated A $\beta_{1-42}$ -Induced Oxidative Stress and A $\beta$ Peptide Levels in N2a Cells

The levels of oxidative stress in N2a cells in various groups were tested by measuring intracellular levels of ROS, SOD and MDA. Compared with the control group, 10  $\mu$ M A $\beta_{1-42}$  gave rise to a prominent reduction of SOD

level and a considerable elevation of ROS and MDA levels (Fig. 2a-c). On the contrary, 100  $\mu$ M GB pretreatment significantly relieved A $\beta_{1-42}$ -induced oxidative injury with increased SOD level and decreased ROS and MDA levels (Fig. 2a-c). Then, we examined whether GB affects A $\beta_{1-42}$  peptide expression. Western blot revealed that A $\beta_{1-42}$  peptide level significantly increased with A $\beta_{1-42}$  intervention, and the uptrend was reversed by 100  $\mu$ M GB pretreatment (Fig. 2d).

### 3.4 Global Proteome Profiling of N2a Cells with GB Pretreatment

To explore the neuroprotective mechanisms of GB against cell injury stimulated by  $A\beta_{1-42}$  oligomers, TMT-labeled LC-MS/MS analysis was executed to find out the relative changes in protein abundance. The workflow is exhibited in Fig. 3a. Cells from the control group,  $A\beta$  group and  $A\beta$  + GB group were labeled with 126 and 127 TMT tags, 128 and 129 TMT tags, and 130 and 131 TMT tags, respectively. In the end, 6969 proteins were identified and 6740 proteins (96.71%) were quantified in two independent biological replicates. The relative abundance ratios ( $A\beta$  + GB/ $A\beta$ ) distribution of the quantified proteins was normality (Fig. 3b). Only proteins with fold change  $>1.5$  and  $p$  value  $< 0.1$  were identified to be differentially expressed. 61 proteins were considered as DEPs, including 42 upregulated and 19 downregulated proteins. In the volcano figure, red dots indicate upregulated proteins and blue dots indicate downregulated proteins (Fig. 3c). The DEPs were showed in Table 1.

To identify obviously different proteins in GB treated N2a cells, hierarchical clustering analysis was performed. The heatmap of 61 DEPs revealed that DEPs were distinctly separated into three distinct areas (Fig. 4). The expression levels of DEPs in the  $A\beta$  group were apparently different from those in the control group, while GB pretreatment attenuated these differences. These results indicated that protein expression undergoes extensive remodeling during AD pathogenesis and this trend can be partially reversed by GB.

### 3.5 GO and KEGG Enrichment Analyses of DEPs in $A\beta_{1-42}$ -Induced N2a Cells with GB Pretreatment

To explore the biological classification of the DEPs, we annotated the DEPs into some functional categories using DAVID. These proteins were categorized in accordance with GO biological process (GOBP), GO molecular function (GOMF), GO cellular component (GOCC) and KEGG enrichment analysis by DAVID [25]. GOBP analysis showed that DEPs predominantly participate in response to external stimulation (GO:0032101,  $p = 7.52E-07$ ), immune system process (GO:0002684,  $p = 2.82E-05$ ), cell activation (GO:0001775,  $p = 0.0004$ ), and negative regulation of cell death (GO:0060548,  $p = 0.011$ ) (Fig. 5a). GOMF analysis showed that the DEPs were principally associated with signaling receptor binding (GO:0005102,  $p = 2.02E-05$ ), transition metal ion binding (GO:0046914,  $p = 0.003$ ), and peptidase regulator activity (GO:0061134,  $p = 4.53E-09$ ) (Fig. 5b). In the GOCC analysis, we discovered that most DEPs were localized in the extracellular region (GO:0005576,  $p = 6.99E-18$ ) and extracellular matrix (GO:0031012,  $p = 1.59E-07$ ), followed by cell surface (GO:0009986,  $p = 0.0002$ ) and cell body (GO:0044297,  $p = 0.015$ ) (Fig. 5c). KEGG pathway analysis indicated that the biological pathways were involved in complement and coagulation cascades (mmu04610,  $p = 4.05E-08$ ), ferropto-

sis (mmu04216,  $p = 0.00027$ ), cytokine-cytokine receptor interaction (mmu04060,  $p = 0.0006$ ), and PPAR signaling pathway (mmu03320,  $p = 0.0058$ ) (Fig. 5d).

### 3.6 Validation of the Key Proteins in DEPs

To confirm the MS-based quantitative proteomics, we analyzed the expression levels of two key proteins SPP1 and FTH1 in  $A\beta_{1-42}$ -induced and GB treated N2a cells using western blot and qPCR. FTH1 protein and mRNA levels in the  $A\beta$  group decreased markedly, and 100  $\mu$ M GB treatment upregulated their expressions (Fig. 6b,c). SPP1 protein and mRNA levels in the  $A\beta$  group significantly increased, and these upregulations were potently suppressed by 100  $\mu$ M GB pretreatment (Fig. 6a,c). The change tendency of FTH1 and SPP1 expression levels detected by western blot and qPCR is consistent with mass spectrometric data.

## 4. Discussion

Extracellular aggregated amyloid plaques and intracellular highly phosphorylated neurofibrillary tangles are the typical pathological features of AD. Abnormal aggregation of neurotoxic  $A\beta$  promotes inflammatory responses, oxidative stress, and apoptotic activation, which results in extensive neuron death and the onset of clinical symptoms [26]. GB has anti-apoptotic and antioxidant functions against cerebral ischemic injury and  $A\beta$ -induced neurotoxicity [12,14].  $A\beta$ -induced cell injury model of AD has been widely used for the investigation of AD pathogenesis. In the present study, N2a cells stimulated by  $A\beta_{1-42}$  oligomers alone revealed significantly decreased cell survival rates and cell apoptosis. Nevertheless, this change was efficiently reversed in cells with GB pretreatment (Fig. 1e-g). These results showed that GB relieved cell toxicity and apoptosis caused by  $A\beta_{1-42}$  oligomers, implying the neuroprotective effect of GB against cell injury. Next, we investigated whether GB protects against  $A\beta_{1-42}$ -induced oxidative injury in N2a cells. GB inhibited intracellular ROS and MDA production and induced an upregulation of antioxidant substance like SOD (Fig. 2a-c), demonstrating the antioxidant effect of GB on cell toxicity stimulated by  $A\beta_{1-42}$  oligomers. In addition, the increased  $A\beta$  peptide level in the  $A\beta$  group was also reversed by 100  $\mu$ M GB (Fig. 2d). GB provided anti-apoptotic and antioxidant function on  $A\beta_{1-42}$ -induced cell injury, and downregulated  $A\beta$  peptide expression. However, the potential molecular mechanisms of GB in the progression of AD remain ambiguous.

In order to explore the neuroprotective effects of GB in AD and reveal its underlying molecular mechanisms, TMT labeled proteomics was performed to explore the profile of DEPs associated with GB pretreatment in  $A\beta$ -induced cell injury model of AD (Figs. 3,4). We confirmed 61 DEPs in  $A\beta_{1-42}$ -induced N2a cells with GB pretreatment, including 42 upregulated and 19 downregulated proteins (Table 1).

These DEPs contained several known AD protein biomarkers, like presenilin-2 (PSEN2), SPP1, and SLC7A11. The protein levels of Psen2, SPP1, and SLC7A11 were remarkably increased in A $\beta$  group, and decreased after GB treatment. On the basis of LC-MS/MS analysis results, bioinformatic analysis of DEPs were applied to uncover the underlying signaling pathways and protein targets of GB.

GO enrichment analysis showed that DEPs mainly participated in the regulation of cell death, reminded us that apoptotic signaling pathway has definite function in the pharmacological effects of GB in AD (Fig. 5). Proteins involved in the regulation of cell death pathway included PSEN2 and SPP1. Secreted glycoposphoprotein SPP1 has an extensive range of functions [27], such as prompting neuroinflammation and apoptosis. SPP1 protein expression has been observed to upregulate in the prefrontal cortex and cerebrospinal fluid of AD patients [27,28], as well as in APP/human presenilin-1(PS1) KI mouse model of AD [29]. Our study showed that SPP1 participants in the regulation of apoptotic progress of AD and exacerbates cell apoptosis. We validated obvious up-regulation of SPP1 in A $\beta_{1-42}$ -induced N2a cells, and the increased SPP1 level was significantly reduced after GB treatment (Fig. 6). These results further support the anti-apoptotic effect of GB in AD, which possibly is related to downregulated SPP1 protein.

KEGG enrichment analysis showed that DEPs in GB treated N2a cells were concerned with ferroptosis. Ferroptosis is a newly recognized iron-dependent oxidative cell death that is considered as a crucial pathological process in AD [30,31]. It depends on the regulation of various iron metabolism proteins, such as FTH1 and ferroportin [32]. FTH1, the essential iron storage protein, provides protective effects against neural damage through the regulation of iron metabolism [33,34]. In APP/PS1 mice, neurons in cerebral cortex and hippocampus were vulnerable to ferroptosis, accompanied by downregulated FTH1 protein [30]. GB exerted anti-ferroptosis effects by up-regulating Nrf2 and FTH1 in nonalcoholic fatty liver disease [35]. Consistent with previous conclusions, FTH1 remarkably decreased in the A $\beta$  group and GB pretreatment upregulated its expression in our study (Fig. 6). This result implies that GB may exert anti-ferroptosis effect by up-regulating FTH1 protein in AD.

Taken together, above results confirmed that GB exerts neuroprotective effects against A $\beta_{1-42}$  induced cell injury by restoring DEPs involved in the regulation of cell death and ferroptosis. GB provided anti-apoptotic and anti-ferroptosis roles in AD through down-regulating SPP1 and up-regulating FTH1. Therefore, SPP1 and FTH1 proteins can be considered as potential therapeutic targets of GB for AD.

## 5. Conclusions

In conclusion, the current study demonstrates that GB therapy dramatically attenuates A $\beta_{1-42}$ -induced cell tox-

icity, cell apoptosis and oxidative stress. We identified 42 upregulated and 19 downregulated DEPs in GB treated N2a cells using TMT labeled proteomics. GB provided anti-apoptotic and anti-ferroptosis effects against A $\beta_{1-42}$ -induced cell injury may partly through down-regulating SPP1 protein and up-regulating FTH1 protein. SPP1 and FTH1 proteins are expected to be potential therapeutic targets of GB in AD. Our conclusions were mainly derived from mass spectrometry data and bioinformatic analysis, which must have some limitations. More precise validation and additional study will be performed in the future.

## Abbreviations

ACN, acetonitrile; AGC, automatic gain control; A $\beta$ , amyloid beta; AD, Alzheimer's disease; ANOVA, one-way analysis of variance; APP, amyloid precursor protein; DEPs, differentially expressed proteins; DMEM, Dulbecco's Modified Eagle Medium; DMSO, Dimethyl sulfoxide; FDR, false discovery rate; FITC, fluorescein isothiocyanate; FTH1, ferritin heavy chain 1; GB, Ginkgolide B; GOBP, gene ontology biological process; GOCC, GO cellular component; GOMF, GO molecular function; HRP, horseradish peroxidase; KEGG, Kyoto Encyclopedia of Genes and Genomes; LC-MS/MS, Liquid chromatography-tandem mass spectrometry; MTT, 3,4,5-dimethylthiazol-2-yl-2,5-diphenyl-tetrazolium bromide; PE, phycoerythrin; PI, propidium iodide; PS1, human presenilin-1; PSEN2, presenilin-2; qRT-PCR, quantitative real-time PCR; ROS, reactive oxygen species; SPP1, osteopontin; TFA, trifluoroacetic acid; TEM, transmission electron microscopy; TMT, Tandem mass tag.

## Consent for publication

The manuscript is approved by all authors for publication. We would like to declare on behalf of my co-authors that the manuscript has not been previously published, and is not currently submitted for review to any other journal, and will not be submitted elsewhere before a decision is made by this journal.

## Author Contributions

GFY—conceptualization, methodology and supervision. YDZ—writing - original draft preparation, investigation, and writing - reviewing and editing. YZ—investigation. JZ—validation. YG and SYL—data curation. CC—supervision.

## Ethics Approval and Consent to Participate

Our research was based on N2a cell line, and did not involve human or animals. No ethical approval is required.

## Acknowledgment

Not applicable.

## Funding

This study was supported by a Grant-in-Aid from the Scientific Research Project of Hebei Administration of Traditional Chinese Medicine (2020172).

## Conflict of Interest

The authors declare no conflict of interest.

## References

- [1] Persson T, Popescu BO, Cedazo-Minguez A. Oxidative stress in Alzheimer's disease: why did antioxidant therapy fail? *Oxidative Medicine and Cellular Longevity*. 2014; 2014: 427318.
- [2] Flemmig J, Zámocký M, Alia A. Amyloid  $\beta$  and free heme: bloody new insights into the pathogenesis of Alzheimer's disease. *Neural Regeneration Research*. 2018; 13: 1170–1174.
- [3] Blennow K, de Leon MJ, Zetterberg H. Alzheimer's disease. *The Lancet*. 2006; 368: 387–403.
- [4] Palop JJ, Mucke L. Amyloid-beta-induced neuronal dysfunction in Alzheimer's disease: from synapses toward neural networks. *Nature Neuroscience*. 2010; 13: 812–818.
- [5] Balducci C, Forloni G. APP Transgenic Mice: their Use and Limitations. *NeuroMolecular Medicine*. 2011; 13: 117–137.
- [6] De Strooper B, Vassar R, Golde T. The secretases: enzymes with therapeutic potential in Alzheimer disease. *Nature Reviews Neurology*. 2010; 6: 99–107.
- [7] Borchelt DR, Thinakaran G, Eckman CB, Lee MK, Davenport F, Ratovitsky T, *et al.* Familial Alzheimer's disease-linked presenilin 1 variants elevate Abeta1-42/1-40 ratio *in vitro* and *in vivo*. *Neuron*. 1996; 17: 1005–1013.
- [8] Surguchov A, Bernal L, Surguchev AA. Phytochemicals as Regulators of Genes Involved in Synucleinopathies. *Biomolecules*. 2021; 11: 624.
- [9] Lenoir M, Pedruzzi E, Rais S, Drieu K, Perianin A. Sensitization of human neutrophil defense activities through activation of platelet-activating factor receptors by ginkgolide B, a bioactive component of the Ginkgo biloba extract EGB 761. *Biochemical Pharmacology*. 2002; 63: 1241–1249.
- [10] Niu YH, Yang XY, Bao WS. Protective effects of Ginkgo biloba extract on cultured rat cardiomyocytes damaged by H<sub>2</sub>O<sub>2</sub>. *Zhongguo Yao Li Xue Bao*. 1999; 20: 635–638.
- [11] Guidetti C, Paracchini S, Lucchini S, Cambieri M, Marzatico F. Prevention of neuronal cell damage induced by oxidative stress *in-vitro*: effect of different Ginkgo biloba extracts. *Journal of Pharmacy and Pharmacology*. 2001; 53: 387–392.
- [12] Gu JH, Ge JB, Li M, Wu F, Zhang W, Qin ZH. Inhibition of NF- $\kappa$ B activation is associated with anti-inflammatory and anti-apoptotic effects of Ginkgolide B in a mouse model of cerebral ischemia/reperfusion injury. *European Journal of Pharmaceutical Sciences*. 2012; 47: 652–660.
- [13] Huang M, Qian Y, Guan T, Huang L, Tang X, Li Y. Different neuroprotective responses of Ginkgolide B and bilobalide, the two Ginkgo components, in ischemic rats with hyperglycemia. *European Journal of Pharmacology*. 2012; 677: 71–76.
- [14] Kaur N, Dhiman M, Perez-Polo JR, Mantha AK. Ginkgolide B revamps neuroprotective role of apurinic/aprimidinic endonuclease 1 and mitochondrial oxidative phosphorylation against A $\beta$ 25-35-induced neurotoxicity in human neuroblastoma cells. *Journal of Neuroscience Research*. 2015; 93: 938–947.
- [15] Aebersold R, Mann M. Mass-spectrometric exploration of proteome structure and function. *Nature*. 2016; 537: 347–355.
- [16] Seger C, Salzmann L. After another decade: LC-MS/MS became routine in clinical diagnostics. *Clinical Biochemistry*. 2020; 82: 2–11.
- [17] Zhang Y, Zhao Y, Zhang J, Gao Y, Li S, Chang C, *et al.* Ginkgolide B inhibits NLRP3 inflammasome activation and promotes microglial M2 polarization in  $\alpha\beta$ 1-42-induced microglia cells. *Neuroscience Letters*. 2021; 764: 136206.
- [18] Dahlgren KN, Manelli AM, Stine WB Jr, Baker LK, Krafft GA, LaDu MJ. Oligomeric and fibrillar species of amyloid-beta peptides differentially affect neuronal viability. *Journal of Biological Chemistry*. 2002; 277: 32046–32053.
- [19] Stine WB, Jungbauer L, Yu C, LaDu MJ. Preparing synthetic A $\beta$  in different aggregation states. *Methods in Molecular Biology*. 2011; 670: 13–32.
- [20] Schniers A, Pasing Y, Hansen T. Lys-C/Trypsin Tandem-Digestion Protocol for Gel-Free Proteomic Analysis of Colon Biopsies. *Methods in Molecular Biology*. 2019; 43: 113–122.
- [21] Elias JE, Gygi SP. Target-Decoy Search Strategy for Mass Spectrometry-Based Proteomics. *Methods in Molecular Biology*. 2010; 5: 55–71.
- [22] Elias JE, Gygi SP. Target-decoy search strategy for increased confidence in large-scale protein identifications by mass spectrometry. *Nature Methods*. 2007; 4: 207–214.
- [23] Huang DW, Sherman BT, Lempicki RA. Systematic and integrative analysis of large gene lists using DAVID bioinformatics resources. *Nature Protocols*. 2009; 4: 44–57.
- [24] Huang DW, Sherman BT, Lempicki RA. Bioinformatics enrichment tools: paths toward the comprehensive functional analysis of large gene lists. *Nucleic Acids Research*. 2009; 37: 1–13.
- [25] Carmona-Saez P, Chagoyen M, Tirado F, Carazo JM, Pascual-Montano A. GENECODIS: a web-based tool for finding significant concurrent annotations in gene lists. *Genome Biology*. 2007; 8: R3.
- [26] Sinyor B, Mineo J, Ochner C. Alzheimer's Disease, Inflammation, and the Role of Antioxidants. *Journal of Alzheimer's Disease Reports*. 2020; 4: 175–183.
- [27] Begcevic I, Brinc D, Brown M, Martinez-Morillo E, Goldhardt O, Grimmer T, *et al.* Brain-related proteins as potential CSF biomarkers of Alzheimer's disease: a targeted mass spectrometry approach. *Journal of Proteomics*. 2018; 182: 12–20.
- [28] Sathe G, Albert M, Darrow J, Saito A, Troncoso J, Pandey A, *et al.* Quantitative proteomic analysis of the frontal cortex in Alzheimer's disease. *Journal of Neurochemistry*. 2021; 156: 988–1002.
- [29] Wirths O, Breyhan H, Marcello A, Cotel M, Brück W, Bayer TA. Inflammatory changes are tightly associated with neurodegeneration in the brain and spinal cord of the APP/PS1KI mouse model of Alzheimer's disease. *Neurobiology of Aging*. 2010; 31: 747–757.
- [30] Gao Y, Li J, Wu Q, Wang S, Yang S, Li X, *et al.* Tetrahydroxy stilbene glycoside ameliorates Alzheimer's disease in APP/PS1 mice via glutathione peroxidase related ferroptosis. *International Immunopharmacology*. 2021; 99: 108002.
- [31] Bao W, Pang P, Zhou X, Hu F, Xiong W, Chen K, *et al.* Loss of ferroportin induces memory impairment by promoting ferroptosis in Alzheimer's disease. *Cell Death & Differentiation*. 2021; 28: 1548–1562.
- [32] Bogdan AR, Miyazawa M, Hashimoto K, Tsuji Y. Regulators of Iron Homeostasis: New Players in Metabolism, Cell Death, and Disease. *Trends in Biochemical Sciences*. 2016; 41: 274–286.
- [33] Tian Y, Lu J, Hao X, Li H, Zhang G, Liu X, *et al.* FTH1 Inhibits Ferroptosis through Ferritinophagy in the 6-OHDA Model of Parkinson's Disease. *Neurotherapeutics*. 2020; 17: 1796–1812.
- [34] Chiba T, Fujita S, Kubota H, Inoue D, Mizuno A, Komatsu T, *et al.* Identification of Fasting-induced Genes in the Rat Hypothalamus: Relationship with Neuroprotection. *Annals of the New York Academy of Sciences*. 2007; 1119: 216–226.
- [35] Yang Y, Chen J, Gao Q, Shan X, Wang J, Lv Z. Study on the attenuated effect of Ginkgolide B on ferroptosis in high fat diet induced nonalcoholic fatty liver disease. *Toxicology*. 2020; 445: 152599.